

1 **Capturing noroviruses circulating in the population: sewage surveillance in Guangdong, China**

2 **(2013–2018)**

3 J. Lu,<sup>1,2,3\*</sup> L. Fang,<sup>2</sup> J.J. Peng,<sup>1,2,3</sup> L.L. Zeng,<sup>1,2</sup> H.F. Lin,<sup>1,2</sup> Q.L. Xiong,<sup>1,2,3</sup> L.N. Yi,<sup>1,2</sup> T. Song,<sup>2</sup> J.F. He,<sup>2</sup>

4 L. M. Sun,<sup>2</sup> C.W. Ke,<sup>2</sup> H. Li,<sup>2</sup> H.Y. Zheng<sup>2\*</sup>

5

6 **Affiliations:**

7 <sup>1</sup> Guangdong Provincial Institution of Public Health, Guangdong Provincial Center for Disease Control

8 and Prevention, Guangzhou, China

9 <sup>2</sup> Guangdong Provincial Center for Disease Control and Prevention, Guangzhou, China

10 <sup>3</sup> School of Public Health, Southern Medical University, Guangzhou, China

11

12 **\*Correspondent to:**

13 Huanying Zheng, email: zhenghy.gdcdc@gmail.com, Guangdong Provincial Center for Disease

14 Control and Prevention, China;

15 Or

16 Jing Lu, email: Jimlu0331@163.com, Guangdong Provincial Institution of Public Health, China;

17

18 **Abstract**

19 Noroviruses (NoVs) are the leading cause of acute gastroenteritis outbreaks. The specific geographical  
20 distribution and expanding diversity of NoVs has posed a challenge to NoV surveillance and  
21 interventions. Here, we describe the long-term dynamic correlation between NoV distribution in  
22 sewage and in the local population by using high-throughput sequencing and operational taxonomic  
23 unit (OTU) analysis. The NoV viral loads in sewage were closely associated with the number of NoV  
24 outbreaks in the population. Compared with the viral distributions in outbreaks, the dominance of the  
25 newly emerged variants, such as GII.P17-GII.17 and GII.P16-GII.2, could be detected two months  
26 ahead in sewage. In addition, the dynamics of pre-epidemic variants, which were rarely detected from  
27 clinics, could be captured through sewage surveillance, thus improving our understanding of the viral  
28 origin and evolution. Our data highlight that the high-throughput environmental screening should  
29 become a critical part of the response to infectious diseases.

30

31 **Introduction**

32 Currently, emerging infectious diseases present one of the greatest public health challenges. Human  
33 noroviruses (NoVs) are recognized as the leading cause of acute gastroenteritis (AGE) for all ages (1).  
34 Viral infections are estimated to be associated with 18% of diarrheal diseases and 212,000 deaths  
35 annually (2). Due to their high contagiousness, most cluster infections or outbreaks of NoVs have been  
36 reported in semienclosed settings such as hospitals, childcare centers, schools, and universities, leading  
37 to public panic regarding disease transmission (3).

38

39 Based on the sequence of the VP1 gene, NoVs can be classified into seven genogroups (GI–GVII) and  
40 further subdivided into more than 40 genotypes (4). Viruses from the GI, GII, and GIV genogroups are  
41 known to infect humans. Currently, there is no drug or licensed vaccine for NoV infections. Disease  
42 control has mainly relied on clinical surveillance, which informs us of the emergence and prevalence of  
43 different genotypes and their potential risks of causing global outbreaks. Since 1995, GII.4 has been  
44 identified as the predominant genotype responsible for 65-80% of NoV infections worldwide (5, 6).  
45 The novel GII.4 variant has emerged every 2-5 years and presented amino acid changes in five  
46 antigenic sites (7) associated with viral escape from herd immunity (8, 9). This epochal evolution  
47 pattern is regarded as the principal mechanism adopted by GII.4 to sustain its predominance and has  
48 led to successive pandemics in the global population (10–12). However, in the winter seasons of  
49 2014-2015 and 2016-2017, novel variants of some genotypes, such as GII.P17-GII.17 and  
50 GII.P16-GII.2, emerged. These NoV genotypes, which were rarely identified previously, have replaced  
51 GII.4 and caused increasing AGE outbreaks in Asia-Pacific regions. The emergence of these novel  
52 variants was also observed in European countries, with a rising prevalence in 2015-2016 (13).

53

54 The temporal and spatial variances in NoV genetic distribution pose a significant challenge to NoV  
55 vaccine design and for early warning of NoV outbreaks, for which more extensive and timely  
56 surveillance is warranted. In this study, we developed a high-throughput method to capture NoVs in  
57 sewage. With this method, the dynamics of NoV distribution in Guangzhou sewage were investigated  
58 from 2013 to 2018. The corresponding epidemiological data of NoV outbreaks were subtracted from  
59 the clinical surveillance network to evaluate how sewage data could improve our knowledge of NoV  
60 circulation in the population, especially for early detection of novel NoV variants.

## 61 **Results**

### 62 **Norovirus genotype distributions in AGE outbreaks, 2013-2018**

63 The Guangdong provincial surveillance network was launched in 2013 for monitoring AGE outbreaks  
64 in 21 prefectural cities (14). In total, 327 NoV-associated outbreaks were reported between January  
65 2013 and December 2018. The majority of these outbreaks (284 of 327, 87%) were caused by the GII  
66 genogroup, in which GII.4, GII.17, GII.2, and GII.3 were the predominant genotypes, causing 24, 75,  
67 143 and 42 outbreaks, respectively. As previously reported, a novel variant of GII.17 (GII.P17-GII.17)  
68 (14) and a recombinant variant GII.2 (GII.P16-GII.2) (15) emerged in Guangdong in 2015 and 2017,  
69 respectively. These novel variants caused a significant increase (>4-fold) in AGE outbreaks and  
70 became predominant in the next 2 or 3 years (Fig. 1A). More importantly, the novel variant outbreaks  
71 occurred almost simultaneously in multiple cities, and the epidemic peaked in the following 1-2 months.  
72 In this context, an optimized surveillance system that could provide timely and extensive molecular  
73 surveillance data is warranted.

74

### 75 **Molecular surveillance of norovirus in raw sewage in Guangzhou, 2013-18**

76 Guangzhou is the capital city of Guangdong Province and one of the most populous regions in China.  
77 Between 2013-2018, Guangzhou reported the largest number of NoV outbreaks (72 of 327, 22%, Fig.  
78 1B) and was regarded as an epidemiological hub for NoV transmission (16). Sewage surveillance in  
79 Guangzhou was previously established for the global eradication of poliovirus and was also applied to  
80 investigate the potential origins of enterovirus outbreaks (Lu et al., 2020). To explore the dynamic  
81 correlations of NoV in sewage and in clinical outbreaks, a total of 72 sewage samples were collected  
82 from the Guangzhou wastewater treatment plant (WWTP) each month from January 2013 to December  
83 2018. GI and GII NoVs were detected in 91.7% (66/72) and 100% (72/72) of the samples by RT-PCR.  
84 The relative virus copies in sewage samples correlated well with the number of NoV outbreaks in the  
85 population, with the most abundant GI and GII NoVs detected at the end of winter and in early spring  
86 (November to April of the next year). GI NoV was detected with relatively high viral loads in sewage  
87 but rarely identified in clinical outbreaks, suggesting that most GI infections may be asymptomatic and  
88 that these viruses circulated undetected in the local population. Although correlation was observed  
89 between the viral loads in sewage and the risks of outbreaks in the community, sewage surveillance  
90 still provided limited information for early warning of NoV outbreaks. For instance, the largest NoV  
91 outbreak was reported in the 2016-17 epidemic season, but the contemporary GII viral copies in  
92 sewage were similar to those in the other epidemic seasons. Therefore, the outbreak of NoV was not  
93 only driven by the viral prevalence in the community but could also be triggered by the emergence and

94 transmission of a novel genetic variant for which herd immunity was lacking. Therefore, establishing a  
95 method to capture the genetic diversity of NoV in sewage is critical for optimizing surveillance.

96

#### 97 **Setup and verification of a high-throughput method**

98 It was expected that a sewage sample would contain different NoV genotypes and even genetic variants  
99 from a specific genotype. Capturing the distribution of multiple genotypes and variants by the  
100 conventional Sanger sequencing/cloning method was a great challenge. In this study, we used amplicon  
101 sequencing and calculated the abundances of different genotypes or variants via an operational  
102 taxonomic unit (OTU) clustering method, which is commonly used to define the taxonomic units of  
103 bacterial species in 16S rRNA sequencing. It was expected that the percentage of different genotypes  
104 or variants would be proportional to the corresponding read number in OTU clusters (Fig.2A, details in  
105 Material and Methods). To verify the accuracy of this method, we constructed four plasmids, including  
106 the genome fragments of the GII.2, GII.3, GII.4, and GII.17 genotypes. The copy numbers of these  
107 plasmids were determined through mass measurements. Serial mixtures (groups 1-3) were obtained by  
108 adding the GII.2, GII.3, GII.4, and GII.17 plasmids at ratios of 1:1:1:1, 1:3:6:9, and 1:10:100:1000 (Fig.  
109 2B). The total amount of plasmid mixture for each group was ~0.02 ng (approximately  $6 \times 10^6$  copies).  
110 These samples were first PCR amplified, sequenced with high-throughput sequencing, and analyzed as  
111 described in the Material and Methods section. As shown in Fig. 3, the sequencing results illustrated  
112 the original genotype distribution well when different genotypes were mixed at a similar ratio. When  
113 the genotype ratio was over 1:10, PCR amplification bias likely occurred, and the genotype with a  
114 lower rate may have been overrepresented (Fig. 2B). In group 3, the ratio calculated from the number  
115 of reads in each genotype cluster was 1:6:64:246, which was basically at the same magnitude in which  
116 the plasmids were mixed (1:10:100:1000). The plasmid with the lowest copies ( $6 \times 10^3$  copies) finally  
117 had 1629 clustered reads. These data suggested that the combination of high-throughput sequencing  
118 and the OTU clustering method could roughly identify the percentages of different genotypes in  
119 sewage without losing sensitivity for detecting low-proportion genotypes.

120

#### 121 **Norovirus genotype distributions in sewage, 2013-2018**

122 We next applied the above method to investigate NoV distribution in Guangzhou sewage from  
123 2013-2018. Approximately 1,000,000 reads (range 112,358–2,947,207) were generated from each  
124 amplicon (Table S2). Genotype distributions in the GI and GII genogroups were determined separately  
125 by measuring the number of reads in each genotype cluster. Genotypes with a percentage less than 0.1%  
126 of total reads were removed. In total, 9 GI genotypes and 15 GII genotypes were identified in sewage

127 water from 2013-2018 (Fig. 3A&3C). For the GI genotype, GI.2, GI.8 and GI.9 were found to be  
128 dominant in sewage samples (percentages were over 30%) but with different temporal distributions  
129 (Fig. 3A & 3B). For the GI genogroup, GI.2 was continuously circulating in the population from 2013  
130 through 2018 (Fig. 3A), and its predominance was significant in the 2017-2018 winter season (Fig. 3B).  
131 In contrast, the GI.8 and GI.9 genotypes were dominant in 2013 but were rarely detected in 2017 and  
132 2018 (Fig. 3A).

133

134 GII NoV was the dominant genogroup causing AGE outbreaks. The temporal pattern of GII genotypes  
135 in sewage was well captured. GII.2, GII.4, and GII.17 were the major circulating genotypes in sewage,  
136 and other genotypes were detected with lower prevalence (<25%, Fig. 3C). More specifically, GII.4  
137 was dominant (> 50%) in 2013 and several months of 2014 but detected at lower level in the winter  
138 season (January to April) from 2015 through 2018. GII.17 was occasionally identified as a dominant  
139 genotype in September 2013, and increasing detection of this genotype was observed in the winter  
140 season of 2014 (Fig. 3D). The percentage of the GII.17 genotype was over 50% in nearly all months  
141 from November 2014 through April 2016, consistent with its dominance in the outbreaks (Fig. 1). GII.2  
142 was detected at a relatively low level before mid-2016 but has been increasingly identified since  
143 October 2016. Interestingly, the high prevalence of GII.4 in sewage was only observed in months  
144 before epidemic seasons (mainly July to December), and this dominance was quickly taken over by  
145 GII.17 or GII.2 in all the epidemic seasons from 2014-2018 (Fig. 3D). These data suggested that  
146 compared to GII.4, the newly emerged variants of GII.17 and GII.2 likely have higher transmission  
147 efficiency when etiological factors are favorable.

148

#### 149 **Phylogenetic analyses**

150 The emergence and spread of new NoV variants always lead to an increase in NoV outbreaks in the  
151 population. One priority of sewage surveillance is to identify the early emergence of novel genetic  
152 variants and characterize their dynamic distributions. In this study, we set the sequence similarity  
153 threshold at 97% in the clustering method to distinguish the different genetic variants (see Material and  
154 Methods for details). Through this method, we obtained a consensus sequence of a genetic cluster and  
155 the number of reads in it, which was proportional to the abundance in sewage. To define these genetic  
156 clusters, we constructed maximum-likelihood (ML) trees for the GII.2, GII.17 and GII.4 genotypes by  
157 combining all consensus sequences recovered from sewage and representative variant sequences from  
158 public databases (Fig.S1&S2&S3). The 350-bp amplicon sequenced in this study represented one of  
159 the most divergent parts of the viral genome and is widely used for NoV genotyping. For GII.4, nearly

160 all variants identified after 2013 could be classified into the GII.4\_Sydeny2012 lineage (Fig. 4A, top  
161 panel). The GII.4 sequences from sewage between 2013 and 2015 were near the root of the  
162 GII.4\_Sydeny2012 lineage. Notably, two distinct subclusters of GII.4\_Sydeny2012 emerged in August  
163 2016 (Fig. 4A). The GII.4\_Syd12\_Var1 strains started to be detected in sewage in August 2016 and  
164 were more prevalent than other GII.4 variants in the following seasons (Fig. 4A, lower panel). In  
165 addition to the emergence of GII.4\_Syd12\_Var1, GII.4-associated outbreaks increased in winter  
166 2016-17 compared to the low epidemic level observed in 2014 and 2015 (Fig. 4A). Phylogenetic  
167 analysis showed that the GII.4\_Syd12\_Var1 strains were closely related to the  
168 GII.Pe-GII.4\_Sydeny2012 identified in global through the NoroNet network(19). The contemporary  
169 increasing epidemic observed at the end of 2016 highlighted that further characterizing the antigenicity  
170 of GII.4\_Syd12\_Var1 strains and their prevalence in other regions are warranted to evaluate their  
171 epidemic risk. The GII.4\_Syd12\_Var2 strains were closely related to the GII.P16-GII.4\_Sydeny2012  
172 strains recently reported in Europe and America (20–22). GII.P16-GII.4\_Sydeny2012 is associated  
173 with the emergence of the novel recombinant strains GII.P16-GII.2 detected at the end of 2016 (23,  
174 24).

175

176

177 The GII.17 variant was first identified in sewage samples in September 2013, and this variant was  
178 closely related to the pre-epidemic lineage (Kawaski323-like virus) (25). The epidemic variant of  
179 GII.17 (Kawaski308-like virus) was first detected in sewage in September 2014, which was two  
180 months before the occurrence of AGE outbreaks. Notably, in the sewage samples, we found a GII.17  
181 genetic variant (GII.17 variant1) that was close to the GII.Pe-GII.17 viruses recently reported in Hong  
182 Kong (KT589391\_CUHK-NS-682\_HK\_2015-06) and southern Brazil (26) (Fig. 4B). This variant  
183 represented a distinct lineage originating from prototype strain JN699043\_GF\_1978, and it had not  
184 been identified from the outbreaks but was frequently detected in sewage between 2016 and 2018,  
185 indicative of its hidden circulation in the local community.

186

187 For GII.2, four genetic clusters were observed based on the surveillance data, and most of the GII.2  
188 strains in sewage fell into the Var1 and Var2 clades. The Var1 clade, including the dominant strain in  
189 sewage in 2016-2018, represented the epidemic lineage GII.P16-GII.2. This lineage was regarded as a  
190 recombinant of GII.2 and GII.P16-GII.4 and caused outbreaks in multiple regions in 2016 (23, 24, 27).  
191 The Var2 clade included GII.2 strains mainly circulating in sewage between 2013 and 2015. Consistent  
192 with this, the closely related reference sequences for Var2 were identified in Asian-Pacific countries

193 between 2012 and 2015 (Fig. 4C upper panel). The dynamic distribution showed that the percentage of  
194 Var2 fluctuated at a relatively low level (<25%, Fig. 4C lower panel) in sewage in 2013-2015, and this  
195 variant rarely caused outbreaks in the community. In contrast, Var1, representing the 2016 epidemic  
196 strains, was first detected in sewage in September 2016, and its percentage steadily increased in the  
197 following three months. The first occurrence of GII.P16-GII.2 in outbreak surveillance was in  
198 November 2016, which was two months after its dominance in the sewage sample.

199 **Discussion**

200 Currently, multiple NoV genotypes are cocirculating worldwide with continuous and rapid changes in  
201 NoV genetic diversity (13). In contrast to the global predominance of GII.4 observed in the past decade,  
202 the distribution of NoV genotypes is now varied among countries, indicating that spatial and temporal  
203 differences exist. Due to this remarkable change, regional surveillance data are critical for early  
204 warning and vaccine design, similar to the actions taken in response to seasonal influenza viruses. To  
205 date, extensive and timely clinical surveillance is difficult to achieve in most regions. In this study, we  
206 prove that high-throughput sequencing combined with the OTU clustering method could be  
207 successfully applied to investigate the dynamic distribution of NoVs in sewage. By comparison with  
208 long-term surveillance data from NoV outbreaks, our results highlight that sewage surveillance serves  
209 as an efficient tool to capture the NoV distribution in the specific population.

210

211 The current international or regional NoV surveillance networks mostly focus on AGE outbreaks or  
212 sporadic infections from clinics. As a member of CaliciNet (3), the Guangdong provincial surveillance  
213 system followed a similar scheme to report NoV-associated AGE outbreaks in 21 prefectural cities.  
214 Great efforts have been made toward sequencing and molecular typing to capture genotype  
215 distributions, especially for the emerging novel genetic variants in the local population (14, 15).  
216 Several limitations have been found for the current surveillance system. The sporadic infections  
217 reported by sentinel hospitals are often biased, toward the detection of NoV genotypes associated with  
218 a relatively severe symptom. Thus, the method always oversamples specific groups of the population,  
219 such as the young or old age groups and immunocompromised individuals, who tend to have more  
220 severe infections and prolonged symptoms. Outbreak surveillance mostly identifies the genotypes that  
221 may already be efficiently transmitted in the population, and it is difficult to detect those variants  
222 before they are established in the local population. In particular, NoV genotypes such as GII.4 and  
223 GII.17 can have sudden transitions in their antigenicity or infectivity through a few amino acid  
224 mutations in their structural proteins (28–30). Before the transitions, the variants may have limited  
225 infectivity and circulate in the population at a relatively low level. These variants were challenging to  
226 identify during the early stage based on the conventional clinical surveillance system. For example, the  
227 pre-epidemic GII.P17\_GII.17 strains had already disseminated in Guangdong in the early winter of  
228 2013-2014 (Fig. 4B) without any associated AGE outbreaks reported. Several amino acid substitutions  
229 in the antigenic region of VP1 emerged almost simultaneously in the pre-epidemic GII.p17\_GII.17  
230 strain, resulting in the emergence of GII.p17\_GII.17 epidemic strains at the end of 2014 (Fig.4B). This  
231 lineage replaced GII.4 as the predominant genotype and caused AGE outbreaks in Asian-Pacific

232 regions in 2014-2015 (31-33). A similar pattern was also observed for GII.P16\_GII.2, which was  
233 almost simultaneously identified in Germany and multiple areas in China at the end of 2016 (15, 34)  
234 and led to an exponential increase in NoV outbreaks (Fig. 4C). From this perspective, the time window  
235 for our response to the epidemic is too short when we rely on the current clinical surveillance system.

236

237 In this study, we discuss the possibility of capturing the NoV distribution in the local population  
238 through sewage surveillance in a hub city. Before this study, several groups tried to use Sanger  
239 sequencing/cloning or NGS to investigate NoV genotype diversity and temporal dynamics in sewage  
240 (35-37). However, a high-throughput method for calculating the relative abundance of different  
241 genotypes and genetic variants in sewage has not been established. The central question regarding the  
242 dynamic relationship between NoVs in sewage and the human population has still not been adequately  
243 addressed. In this study, the OTU method, which has previously been used for bacterial typing and  
244 distribution counting, was successfully applied for measuring the NoV distribution in sewage. The  
245 study results support sewage surveillance as an efficient way to capture the dynamic distribution of  
246 NoVs in the population nearly in real time (high-throughput sequencing and analyzing could be  
247 completed in 24 hours). First, the correlation between the relative viral loads in sewage and the number  
248 of outbreaks in the community suggests that the viral RNA concentration in sewage is an indicator of  
249 outbreak risks. Second, the dynamics of the novel genetic variants in sewage could be used as a  
250 warning of outbreaks in the population. For example, the epidemic strain GII.P17-GII.17 was dominant  
251 in the sewage sample in September 2014, and the increasing prevalence of this variant in October and  
252 November highlights its outbreak risk in the following epidemic season (Fig. 4B). This pattern was  
253 repeatedly observed two years later, during the outbreak of GII.P16-GII.2 (Fig. 4C). More importantly,  
254 via the clustering method, we could reveal the evolutionary history of these genetic variants, which was  
255 difficult to fully capture by clinical surveillance. As shown in Fig. 4B, the pre-epidemic GII.P17-GII.17  
256 variant was rarely detected in clinics, possibly due to asymptomatic infections. In contrast, this variant  
257 was dominant in sewage in September 2013 and May 2014, with percentages reaching 50% and 75%,  
258 respectively. The establishment of a pre-epidemic strain in the local population provides a foundation  
259 for generating the epidemic GII.P17-GII.17 variant several months later. Similarly, the emergence and  
260 prevalence of GII.P16-GII.4-like strains identified in sewage in the middle of 2016 support the  
261 following recombination identified between GII.P16-GII.4 and GII.2 viruses.

262

263 There remain some limitations to the present study. First, specific PCR amplification is required before  
264 high-throughput sequencing, and the PCR bias would lead to low-proportion (<10%) samples being

265 overrepresented (Fig. 2B). However, we need to balance the sensitivity and precision of this  
266 high-throughput method. The RT-PCR results showed a relatively low copy of NoVs in the raw sewage  
267 (90% samples less than  $3.1 \times 10^5$  copies/L), and direct metagenomic sequencing could obtain only a few  
268 fragments of the most abundant genotype(s). Therefore, PCR amplification is required to analyze the  
269 distribution of multiple genotypes in sewage, especially during the non-epidemic season. Second, the  
270 modified primer set G2SKF and G2SKR was used in this study to produce an ~350-bp fragment  
271 covering part of the VP1 region. From the sequencing data, we could not determine the RdRp genotype  
272 of NoV in sewage. Currently, it remains challenging to find a general primer set for amplifying the  
273 RdRp and VP1 fragments simultaneously, especially because this primer set should have a similar  
274 amplification efficiency among different NoV genotypes. Additionally, limited by the sequence length  
275 of the Illumina sequencing platform, the long fragment could not be sequenced without fragmentation.

276

277 For viral infectious diseases, the surveillance system is designed to answer a set of questions that are  
278 central to disease mitigation and control. These questions include what the virus is, whether it is  
279 genetically different, and how the kinetics of disease transmission are in different populations (38, 39).  
280 Sometimes, clinical surveillance provides a short time window for us to answer these questions and  
281 respond in an informed manner before the occurrence of large outbreaks or exponential growth of the  
282 epidemic. The global pandemic of COVID-19 is another example of how extensive clinical  
283 surveillance is needed for early warning of infectious disease epidemics. Recent sewage surveillance  
284 performed in multiple regions indicated that SARS-CoV-2 RNA could be detected in sewage before  
285 the first COVID-19 cases were reported by local clinical surveillance, and SARS-CoV-2 RNA  
286 concentration in sewage served as a leading indicator of community infection (40, 41). These data  
287 again highlight the importance of sewage surveillance in the early warning of emerging infectious  
288 diseases. With the significant advancement of sequencing technologies, viral disease surveillance has  
289 finally reached a point where high-throughput screening of the associated environmental samples,  
290 including sewage, air, and soil, can become a critical part of the response to infectious diseases.

291

292 **Material and Methods**

293 **Norovirus outbreak surveillance system**

294 The Guangdong provincial AGE outbreak surveillance network has been established since 2013 for  
295 monitoring AGE outbreaks in all 21 cities in Guangdong, China. An outbreak with a cluster of at least  
296 20 AGE cases (meeting the Kaplan criterion) within 3 days must be reported to Guangdong Provincial  
297 Center for Disease Control and Prevention. Samples from each outbreak were first tested for NoV  
298 (Norovirus RT-PCR Kit; Shanghai ZJ Bio-Tech Co., Ltd., China) and for intestinal bacteria at the local  
299 Centers for Disease Control and Prevention. The NoV-positive specimens were delivered to the  
300 Guangdong Provincial Center for Disease Control and Prevention for further genotyping.

301

302 **Sewage surveillance**

303 Raw sewage samples were collected monthly from January 2013 to December 2018 from the primary  
304 sedimentation tanks at the Liede wastewater treatment plant (WWTP) in Guangzhou city, China. This  
305 WWTP serves a population of approximately 2,150,000. A four-liter sample was obtained from the  
306 inlets of the primary sedimentation tanks on a routine basis each month. The sample was immediately  
307 transported to the laboratory, and sample treatment was started within 2 h after the samples arrived at  
308 the laboratory. Viruses in the sewage samples were concentrated using an improved negative-charge  
309 filter membrane absorption and sonication method, as previously described (18). Briefly, the collected  
310 sewage samples were centrifuged at 3,000 rpm for 30 min. Then, MgCl<sub>2</sub> was added to the supernatant  
311 at a final concentration of 0.05 M, and the pH was adjusted to 3.5 to 4.0 with HCl. The samples were  
312 then slowly passed through a negatively charged membrane filter (mixed cellulose ester membrane  
313 filter; Advantec Co. Ltd., Japan) under gentle positive pressure. To elute the viruses, the filter with  
314 adsorbed viruses was cut into pieces and sonicated for 1 min in 10 ml of a 3% beef extract solution (pH  
315 9.6), followed by centrifugation at 1,940 x g for 30 min to yield 8 ml of eluents. Finally, the eluents  
316 were passed through a 0.22 μm syringe filter to remove bacteria and fungi.

317

318 **NGS and bioinformatic analysis**

319 The nucleic acids were extracted from 140 μl of concentrated sewage with a QIAamp Viral RNA  
320 Minikit (Qiagen, USA). RT-PCR was performed with Superscript III (Thermo Fisher, USA) by using  
321 random primers. The cDNA was then used in the first round of PCR amplification with the primer set  
322 described in Table S1. After 27 cycles of amplification, 2.5 μl of the first PCR products were used as a  
323 template in the second-round PCR. After 35 cycles of amplification, the positive products (~354  
324 nucleotides) were subjected to Illumina MiSeq sequencing (PE250), and approximately 1,000,000

325 reads were generated for each PCR product. The datasets were quality controlled (QC) using fastp (42)  
326 to trim artificial sequences (adapters), to cut low-quality bases (quality scores  $<30$ ) and to remove  
327 short reads ( $<50$  bp). Paired-end reads were assembled and PCR primers were trimmed by using  
328 cutadapt. Then, the sequences were clustered into OTUs with the following clustering criteria: 1) all  
329 pairs of OTU sequences should have  $<97\%$  pairwise sequence identity; 2) an OTU sequence should be  
330 the most abundant within a 97% neighborhood. These criteria have been tested to distinguish the  
331 different genetic variants of the NoV genotype, including GII.4, GII.17, and GII.2. After clustering,  
332 genotype assignment was performed using blastn (43) by alignment with the local NoV nucleotide  
333 database. The abundance of different OTUs and genotypes was calculated with the relative number of  
334 raw reads using R scripts. All sequencing metadata generated in this study have been submitted to the  
335 National Genomics Data Center (<https://bigd.big.ac.cn/>) with submission number subCRA003702.

336

### 337 **Phylogenetic analysis**

338 The phylogenetic analyses were performed by combining the partial VP1 gene sequences generated  
339 from sewage samples and the selected reference sequences from the public database (Fig. S1&S2&S3)  
340 to classify the different genetic lineages. ML trees were estimated for sequences from GII.4, GII.17,  
341 and GII.2 by using IQ-Tree (44). Phylogenetic trees were annotated and visualized with ggtree (45).  
342 The dynamic changes in different genetic lineages were visualized using R scripts.

343 **References**

- 344 1. R. L. Atmar, M. K. Estes, The epidemiologic and clinical importance of norovirus infection.  
345 *Gastroenterol. Clin. North Am.* **35**, 275–290, viii (2006).
- 346 2. S. M. Pires, C. L. Fischer-Walker, C. F. Lanata, B. Devleeschauwer, A. J. Hall, M. D. Kirk, A. S.  
347 R. Duarte, R. E. Black, F. J. Angulo, Aetiology-Specific Estimates of the Global and Regional  
348 Incidence and Mortality of Diarrhoeal Diseases Commonly Transmitted through Food. *PLoS*  
349 *ONE*. **10**, e0142927 (2015).
- 350 3. A. J. Hall, M. E. Wikswo, K. Manikonda, V. A. Roberts, J. S. Yoder, L. H. Gould, Acute  
351 gastroenteritis surveillance through the National Outbreak Reporting System, United States.  
352 *Emerging Infect. Dis.* **19**, 1305–1309 (2013).
- 353 4. A. Kroneman, E. Vega, H. Vennema, J. Vinjé, P. A. White, G. Hansman, K. Green, V. Martella, K.  
354 Katayama, M. Koopmans, Proposal for a unified norovirus nomenclature and genotyping.  
355 *Archives of Virology*. **158**, 2059–2068 (2013).
- 356 5. J. J. Siebenga, H. Vennema, D.-P. Zheng, J. Vinjé, B. E. Lee, X.-L. Pang, E. C. M. Ho, W. Lim, A.  
357 Choudekar, S. Broor, T. Halperin, N. B. G. Rasool, J. Hewitt, G. E. Greening, M. Jin, Z.-J. Duan,  
358 Y. Lucero, M. O’Ryan, M. Hoehne, E. Schreier, R. M. Ratcliff, P. A. White, N. Iritani, G. Reuter,  
359 M. Koopmans, Norovirus Illness Is a Global Problem: Emergence and Spread of Norovirus GII.4  
360 Variants, 2001–2007. *J Infect Dis.* **200**, 802–812 (2009).
- 361 6. E. Vega, L. Barclay, N. Gregoricus, S. H. Shirley, D. Lee, J. Vinjé, Genotypic and Epidemiologic  
362 Trends of Norovirus Outbreaks in the United States, 2009 to 2013. *Journal of Clinical*  
363 *Microbiology*. **52**, 147–155 (2014).
- 364 7. K. Tohma, C. J. Lepore, Y. Gao, L. A. Ford-Siltz, G. I. Parra, Population Genomics of GII.4  
365 Noroviruses Reveal Complex Diversification and New Antigenic Sites Involved in the  
366 Emergence of Pandemic Strains. *mBio*. **10** (2019), doi:10.1128/mBio.02202-19.
- 367 8. G. I. Parra, E. J. Abente, C. Sandoval-Jaime, S. V. Sosnovtsev, K. Bok, K. Y. Green, Multiple  
368 Antigenic Sites Are Involved in Blocking the Interaction of GII.4 Norovirus Capsid with ABH  
369 Histo-Blood Group Antigens. *Journal of Virology*. **86**, 7414–7426 (2012).
- 370 9. K. Debbink, E. F. Donaldson, L. C. Lindesmith, R. S. Baric, Genetic Mapping of a Highly

- 371 Variable Norovirus GII.4 Blockade Epitope: Potential Role in Escape from Human Herd  
372 Immunity. *Journal of Virology*. **86**, 1214–1226 (2012).
- 373 10. L. C. Lindesmith, E. F. Donaldson, A. D. LoBue, J. L. Cannon, D.-P. Zheng, J. Vinje, R. S. Baric,  
374 Mechanisms of GII.4 Norovirus Persistence in Human Populations. *PLoS Medicine*. **5**, e31  
375 (2008).
- 376 11. K. Debbink, L. C. Lindesmith, E. F. Donaldson, R. S. Baric, Norovirus Immunity and the Great  
377 Escape. *PLoS Pathogens*. **8**, e1002921 (2012).
- 378 12. J. J. Siebenga, H. Vennema, B. Renckens, E. de Bruin, B. van der Veer, R. J. Siezen, M.  
379 Koopmans, Epochal Evolution of GII.4 Norovirus Capsid Proteins from 1995 to 2006. *Journal*  
380 *of Virology*. **81**, 9932–9941 (2007).
- 381 13. J. van Beek, M. de Graaf, H. Al-Hello, D. J. Allen, K. Ambert-Balay, N. Botteldoorn, M.  
382 Brytting, J. Buesa, M. Cabrerizo, M. Chan, F. Cloak, I. Di Bartolo, S. Guix, J. Hewitt, N. Iritani,  
383 M. Jin, R. Johne, I. Lederer, J. Mans, V. Martella, L. Maunula, G. McAllister, S. Niendorf, H. G.  
384 Niesters, A. T. Podkolzin, M. Poljsak-Prijatelj, L. D. Rasmussen, G. Reuter, G. Tuite, A.  
385 Kroneman, H. Vennema, M. P. G. Koopmans, Molecular surveillance of norovirus, 2005–16: an  
386 epidemiological analysis of data collected from the NoroNet network. *The Lancet Infectious*  
387 *Diseases* (2018), doi:10.1016/S1473-3099(18)30059-8.
- 388 14. J. Lu, L. Sun, L. Fang, F. Yang, Y. Mo, J. Lao, H. Zheng, X. Tan, H. Lin, S. Rutherford, L. Guo,  
389 C. Ke, L. Hui, Gastroenteritis Outbreaks Caused by Norovirus GII.17, Guangdong Province,  
390 China, 2014–2015. *Emerging Infectious Diseases*. **21**, 1240–1242 (2015).
- 391 15. J. Lu, L. Fang, L. Sun, H. Zeng, Y. Li, H. Zheng, S. Wu, F. Yang, T. Song, J. Lin, C. Ke, Y.  
392 Zhang, J. Vinjé, H. Li, Association of GII.P16-GII.2 Recombinant Norovirus Strain with  
393 Increased Norovirus Outbreaks, Guangdong, China, 2016. *Emerging Infectious Diseases*. **23**,  
394 1188–1190 (2017).
- 395 16. J. Lu, L. Fang, H. Zheng, J. Lao, F. Yang, L. Sun, J. Xiao, J. Lin, T. Song, T. Ni, J. Raghvani, C.  
396 Ke, N. R. Faria, T. A. Bowden, O. G. Pybus, H. Li, The Evolution and Transmission of Epidemic  
397 GII.17 Noroviruses. *Journal of Infectious Diseases*. **214**, 556–564 (2016).
- 398 17. J. Lu, M. Kang, H. Zeng, Y. Zhong, L. Fang, X. Zheng, L. Liu, L. Yi, H. Lin, J. Peng, C. Li, Y.

- 399 Zhang, L. Sun, S. Luo, J. Xiao, B. B. O. Munnink, M. P. G. Koopmans, J. Wu, Y. Zhang, Y.  
400 Zhang, T. Song, H. Li, H. Zheng, Tracking echovirus eleven outbreaks in Guangdong, China: a  
401 metatranscriptomic, phylogenetic, and epidemiological study. *Virus Evol.* **6** (2020),  
402 doi:10.1093/ve/veaa029.
- 403 18. H. Zheng, J. Lu, Y. Zhang, H. Yoshida, X. Guo, L. Liu, H. Li, H. Zeng, L. Fang, Y. Mo, L. Yi, T.  
404 Chosa, W. Xu, C. Ke, Prevalence of Nonpolio Enteroviruses in the Sewage of Guangzhou City,  
405 China, from 2009 to 2012. *Applied and Environmental Microbiology.* **79**, 7679–7683 (2013).
- 406 19. J. van Beek, M. de Graaf, H. Al-Hello, D. J. Allen, K. Ambert-Balay, N. Botteldoorn, M.  
407 Brytting, J. Buesa, M. Cabrerizo, M. Chan, F. Cloak, I. D. Bartolo, S. Guix, J. Hewitt, N. Iritani,  
408 M. Jin, R. Johne, I. Lederer, J. Mans, V. Martella, L. Maunula, G. McAllister, S. Niendorf, H. G.  
409 Niesters, A. T. Podkolzin, M. Poljsak-Prijatelj, L. D. Rasmussen, G. Reuter, G. Tuite, A.  
410 Kroneman, H. Vennema, M. P. G. Koopmans, Molecular surveillance of norovirus, 2005–16: an  
411 epidemiological analysis of data collected from the NoroNet network. *The Lancet Infectious*  
412 *Diseases.* **18**, 545–553 (2018).
- 413 20. L. Barclay, J. L. Cannon, M. E. Wikswo, A. R. Phillips, H. Browne, A. M. Montmayeur, R. L.  
414 Tatusov, R. M. Burke, A. J. Hall, J. Vinjé, Emerging Novel GII.P16 Noroviruses Associated with  
415 Multiple Capsid Genotypes. *Viruses.* **11** (2019), doi:10.3390/v11060535.
- 416 21. M. Bidalot, L. Théry, J. Kaplon, A. De Rougemont, K. Ambert-Balay, Emergence of new  
417 recombinant noroviruses GII.p16-GII.4 and GII.p16-GII.2, France, winter 2016 to 2017. *Euro*  
418 *Surveill.* **22** (2017), doi:10.2807/1560-7917.ES.2017.22.15.30508.
- 419 22. M. C. Medici, F. Tummolo, V. Martella, F. De Conto, M. C. Arcangeletti, F. Pinardi, F. Ferraglia,  
420 C. Chezzi, A. Calderaro, Emergence of novel recombinant GII.P16\_GII.2 and GII. P16\_GII.4  
421 Sydney 2012 norovirus strains in Italy, winter 2016/2017. *New Microbiol.* **41**, 71–72 (2018).
- 422 23. J. Lu, L. Fang, L. Sun, H. Zeng, Y. Li, H. Zheng, S. Wu, F. Yang, T. Song, J. Lin, C. Ke, Y.  
423 Zhang, J. Vinjé, H. Li, Association of GII.P16-GII.2 Recombinant Norovirus Strain with  
424 Increased Norovirus Outbreaks, Guangdong, China, 2016. *Emerging Infectious Diseases.* **23**,  
425 1188–1190 (2017).
- 426 24. S. Niendorf, S. Jacobsen, M. Faber, A. M. Eis-Hubinger, J. Hofmann, O. Zimmermann, M.  
427 Hohne, C. T. Bock, Steep rise in norovirus cases and emergence of a new recombinant strain

- 428 GII.P16-GII.2, Germany, winter 2016. *Euro surveillance* □: *bulletin Europeen sur les maladies*  
429 *transmissibles* = *European communicable disease bulletin*. **22** (2017),  
430 doi:10.2807/1560-7917.ES.2017.22.4.30447.
- 431 25. Y. Matsushima, M. Ishikawa, T. Shimizu, A. Komane, S. Kasuo, M. Shinohara, K. Nagasawa, H.  
432 Kimura, A. Ryo, N. Okabe, K. Haga, Y. H. Doan, K. Katayama, H. Shimizu, Genetic analyses of  
433 GII.17 norovirus strains in diarrheal disease outbreaks from December 2014 to March 2015 in  
434 Japan reveal a novel polymerase sequence and amino acid substitutions in the capsid region.  
435 *Euro Surveill.* **20** (2015), doi:10.2807/1560-7917.es2015.20.26.21173.
- 436 26. T. M. Fumian, Norovirus Recombinant Strains Isolated from Gastroenteritis Outbreaks in  
437 Southern Brazil, 2004–2011. *PLOS ONE*, 12 (2016).
- 438 27. K. Kwok, S. Niendorf, N. Lee, T.-N. Hung, L.-Y. Chan, S. Jacobsen, E. A. S. Nelson, T. F. Leung,  
439 R. W. M. Lai, P. K. S. Chan, M. C. W. Chan, Increased Detection of Emergent Recombinant  
440 Norovirus GII.P16-GII.2 Strains in Young Adults, Hong Kong, China, 2016–2017. *Emerging*  
441 *Infectious Diseases*. **23**, 1852–1855 (2017).
- 442 28. L. C. Lindesmith, J. F. Kocher, E. F. Donaldson, K. Debbink, M. L. Mallory, E. W. Swann, P. D.  
443 Brewer-Jensen, R. S. Baric, Emergence of Novel Human Norovirus GII.17 Strains Correlates  
444 With Changes in Blockade Antibody Epitopes. *J Infect Dis.* **216**, 1227–1234 (2017).
- 445 29. G. I. Parra, R. B. Squires, C. K. Karangwa, J. A. Johnson, C. J. Lepore, S. V. Sosnovtsev, K. Y.  
446 Green, Static and Evolving Norovirus Genotypes: Implications for Epidemiology and Immunity.  
447 *PLOS Pathogens*. **13**, e1006136 (2017).
- 448 30. Y. Qian, M. Song, X. Jiang, M. Xia, J. Meller, M. Tan, Y. Chen, X. Li, Z. Rao, Structural  
449 Adaptations of Norovirus GII.17/13/21 Lineage through Two Distinct Evolutionary Paths.  
450 *Journal of Virology*. **93** (2018), doi:10.1128/JVI.01655-18.
- 451 31. M. C. W. Chan, N. Lee, T.-N. Hung, K. Kwok, K. Cheung, E. K. Y. Tin, R. W. M. Lai, E. A. S.  
452 Nelson, T. F. Leung, P. K. S. Chan, Rapid emergence and predominance of a broadly recognizing  
453 and fast-evolving norovirus GII.17 variant in late 2014. *Nature Communications*. **6**, 10061  
454 (2015).
- 455 32. J. Lu, L. Sun, L. Fang, F. Yang, Y. Mo, J. Lao, H. Zheng, X. Tan, H. Lin, S. Rutherford, L. Guo,

- 456 C. Ke, L. Hui, Gastroenteritis Outbreaks Caused by Norovirus GII.17, Guangdong Province,  
457 China, 2014–2015. *Emerging Infectious Diseases*. **21**, 1240–1242 (2015).
- 458 33. Y. Matsushima, M. Ishikawa, T. Shimizu, A. Komane, S. Kasuo, M. Shinohara, K. Nagasawa, H.  
459 Kimura, A. Ryo, N. Okabe, K. Haga, Y. Doan, K. Katayama, H. Shimizu, Genetic analyses of  
460 GII.17 norovirus strains in diarrheal disease outbreaks from December 2014 to March 2015 in  
461 Japan reveal a novel polymerase sequence and amino acid substitutions in the capsid region.  
462 *Eurosurveillance*. **20**, 21173 (2015).
- 463 34. Y. Ao, X. Cong, M. Jin, X. Sun, X. Wei, J. Wang, Q. Zhang, J. Song, J. Yu, J. Cui, J. Qi, M. Tan,  
464 Z. Duan, Genetic analysis of re-emerging GII.P16–GII.2 noroviruses in 2016– 2017 in China, 33  
465 (2018).
- 466 35. B. Prevost, F. S. Lucas, K. Ambert-Balay, P. Pothier, L. Moulin, S. Wurtzer, Deciphering the  
467 Diversities of Astroviruses and Noroviruses in Wastewater Treatment Plant Effluents by a  
468 High-Throughput Sequencing Method. *Appl. Environ. Microbiol.* **81**, 7215–7222 (2015).
- 469 36. J. H. Lun, J. Hewitt, A. Sitabkhan, J.-S. Eden, D. Enosi Tuipulotu, N. E. Netzler, L. Morrell, J.  
470 Merif, R. Jones, B. Huang, D. Warrilow, K.-A. Ressler, M. J. Ferson, D. E. Dwyer, J. Kok, W. D.  
471 Rawlinson, D. Deere, N. D. Crosbie, P. A. White, Emerging recombinant noroviruses identified  
472 by clinical and waste water screening. *Emerging Microbes & Infections*. **7** (2018),  
473 doi:10.1038/s41426-018-0047-8.
- 474 37. B. Prevost, F. S. Lucas, A. Goncalves, F. Richard, L. Moulin, S. Wurtzer, Large scale survey of  
475 enteric viruses in river and waste water underlines the health status of the local population.  
476 *Environment International*. **79**, 42–50 (2015).
- 477 38. N. D. Grubaugh, J. T. Ladner, P. Lemey, O. G. Pybus, A. Rambaut, E. C. Holmes, K. G.  
478 Andersen, Tracking virus outbreaks in the twenty-first century. *Nature Microbiology*. **4**, 10–19  
479 (2019).
- 480 39. J. T. Ladner, N. D. Grubaugh, O. G. Pybus, K. G. Andersen, Precision epidemiology for  
481 infectious disease control. *Nature Medicine*. **25**, 206–211 (2019).
- 482 40. J. Peccia, A. Zulli, D. E. Brackney, N. D. Grubaugh, E. H. Kaplan, A. Casanovas-Massana, A. I.  
483 Ko, A. A. Malik, D. Wang, M. Wang, J. L. Warren, D. M. Weinberger, S. B. Omer, *medRxiv*, in

484 press, doi:10.1101/2020.05.19.20105999.

485 41. W. Randazzo, P. Truchado, E. Cuevas-Ferrando, P. Simón, A. Allende, G. Sánchez, SARS-CoV-2  
486 RNA in wastewater anticipated COVID-19 occurrence in a low prevalence area. *Water Research*.  
487 **181**, 115942 (2020).

488 42. S. Chen, Y. Zhou, Y. Chen, J. Gu, fastp: an ultra-fast all-in-one FASTQ preprocessor.  
489 *Bioinformatics*. **34**, i884–i890 (2018).

490 43. C. Camacho, G. Coulouris, V. Avagyan, N. Ma, J. Papadopoulos, K. Bealer, T. L. Madden,  
491 BLAST+: architecture and applications. *BMC Bioinformatics*. **10**, 421 (2009).

492 44. L.-T. Nguyen, H. A. Schmidt, A. von Haeseler, B. Q. Minh, IQ-TREE: A Fast and Effective  
493 Stochastic Algorithm for Estimating Maximum-Likelihood Phylogenies. *Mol Biol Evol*. **32**,  
494 268–274 (2015).

495 45. G. Yu, D. K. Smith, H. Zhu, Y. Guan, T. T.-Y. Lam, ggtree: an r package for visualization and  
496 annotation of phylogenetic trees with their covariates and other associated data. *Methods in*  
497 *Ecology and Evolution*. **8**, 28–36 (2017).

498 46. S. Kojima, T. Kageyama, S. Fukushi, F. B. Hoshino, M. Shinohara, K. Uchida, K. Natori, N.  
499 Takeda, K. Katayama, Genogroup-specific PCR primers for detection of Norwalk-like viruses.  
500 *Journal of virological methods*. **100**, 107–14 (2002).

501

502 **Acknowledgement:** This study was supported by The Key Research and Development Program of  
503 Guangdong Province (2019B111103001) and Science and Technology Planning Project of Guangzhou  
504 (201804010030).

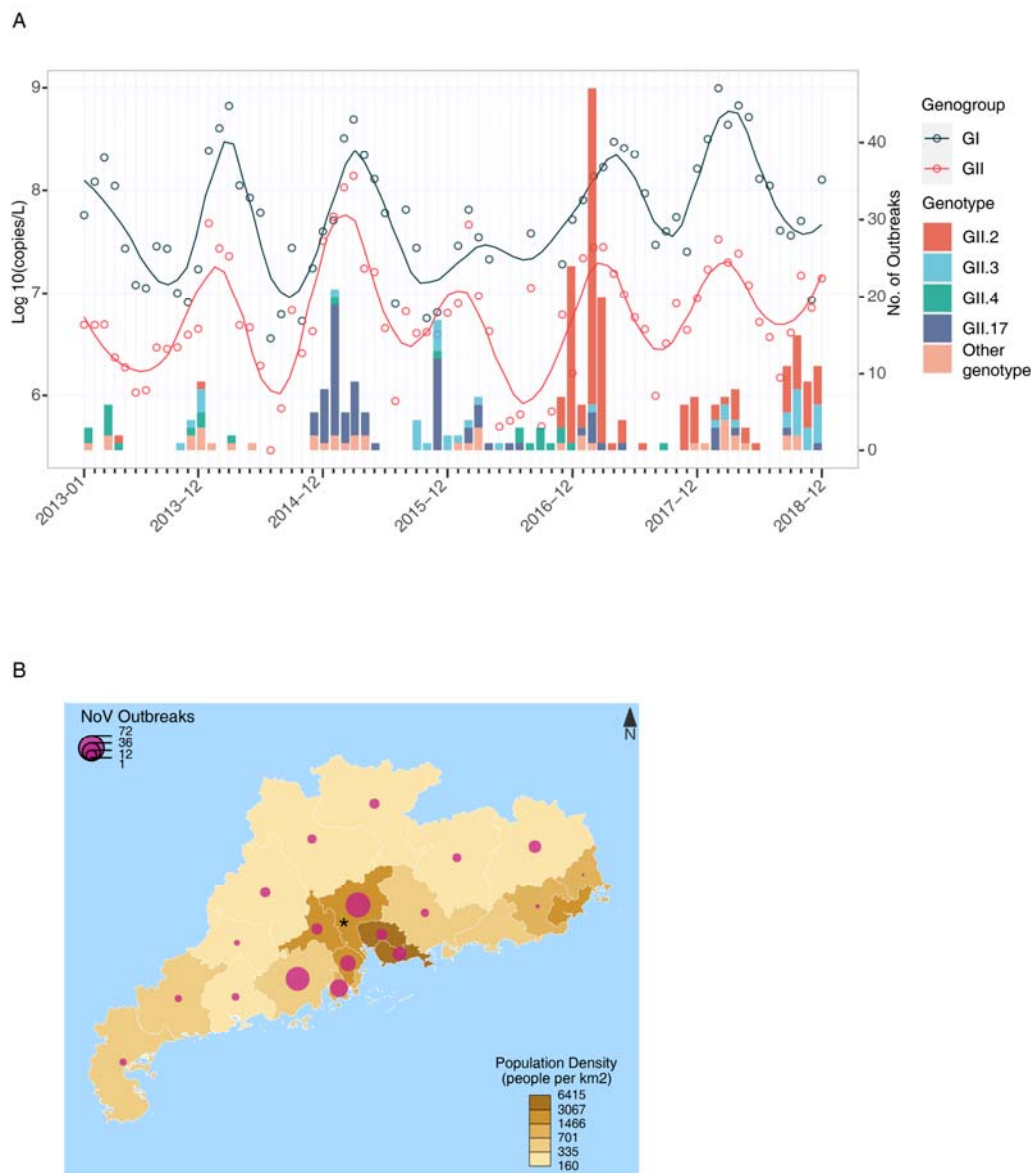
505

506 **Competing interests:** All authors declare no competing interests.

507

508 **Author contributions:** JL designed the study. JL and HYZ had full access to all data in the study, and  
509 take responsibility for the integrity and accuracy of the data. JL, LF, JJP, LLZ, HFL and QLX contributed  
510 to NGS sequencing and the sequences analysis. JL, JJP, LLZ and QLX contributed to literature search  
511 writing of the manuscript. All authors contributed to data acquisition, data interpretation, and all  
512 reviewed and approved the final version of the manuscript.

513 **Figures and Figure legends**



514

515 **Fig. 1. Norovirus outbreaks in Guangdong Province, China, January 2013- December 2018. (A)**

516 Temporal distribution of viral genotypes in norovirus outbreaks. The relative numbers of viral copies of

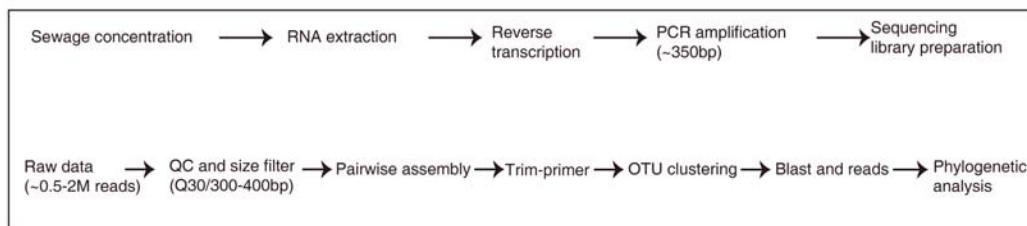
517 GI and GII norovirus in Guangzhou sewage were plotted each month. The samples with viral loads

518 below the detection threshold were set to a Ct-value of 40 ( $<1 \times 10^5$  copies/L) for convenience. (B)

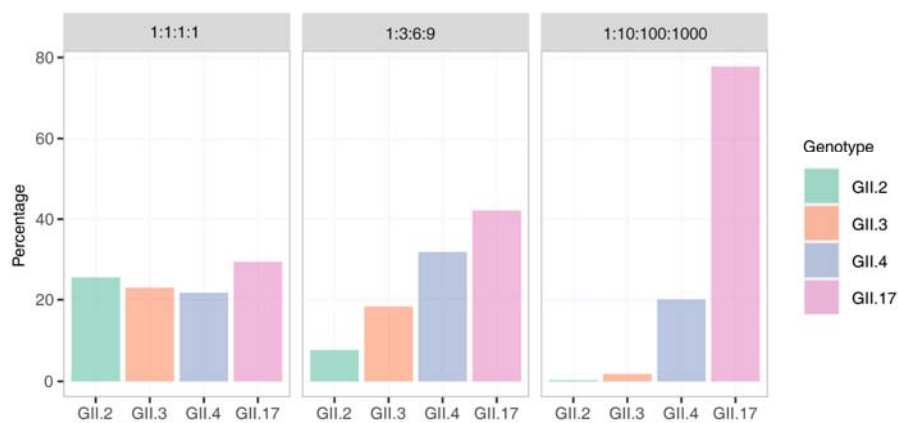
519 Spatial distribution of norovirus outbreaks in 21 prefectural cities in Guangdong, China. Guangzhou,

520 the hub of the norovirus epidemic, is marked with a star.

A



B



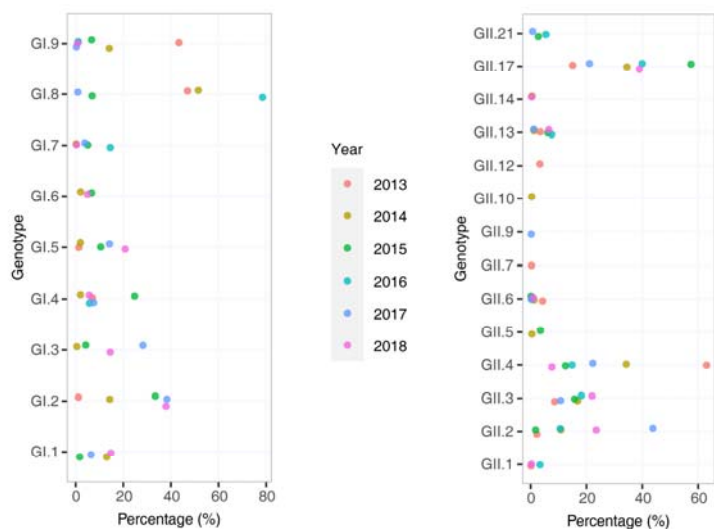
521

522 **Fig. 2. A high-throughput method for detecting NoVs in sewage.** (A) workflow for calculating

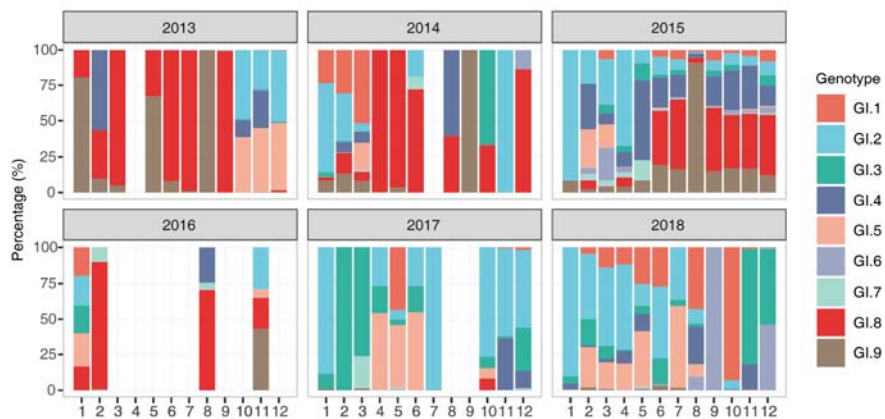
523 genotype distribution in sewage. (B) Method verification by using GII.2, GII.3, GII.4, and GII.17

524 plasmid constructs mixed in different ratios.

A



B



525

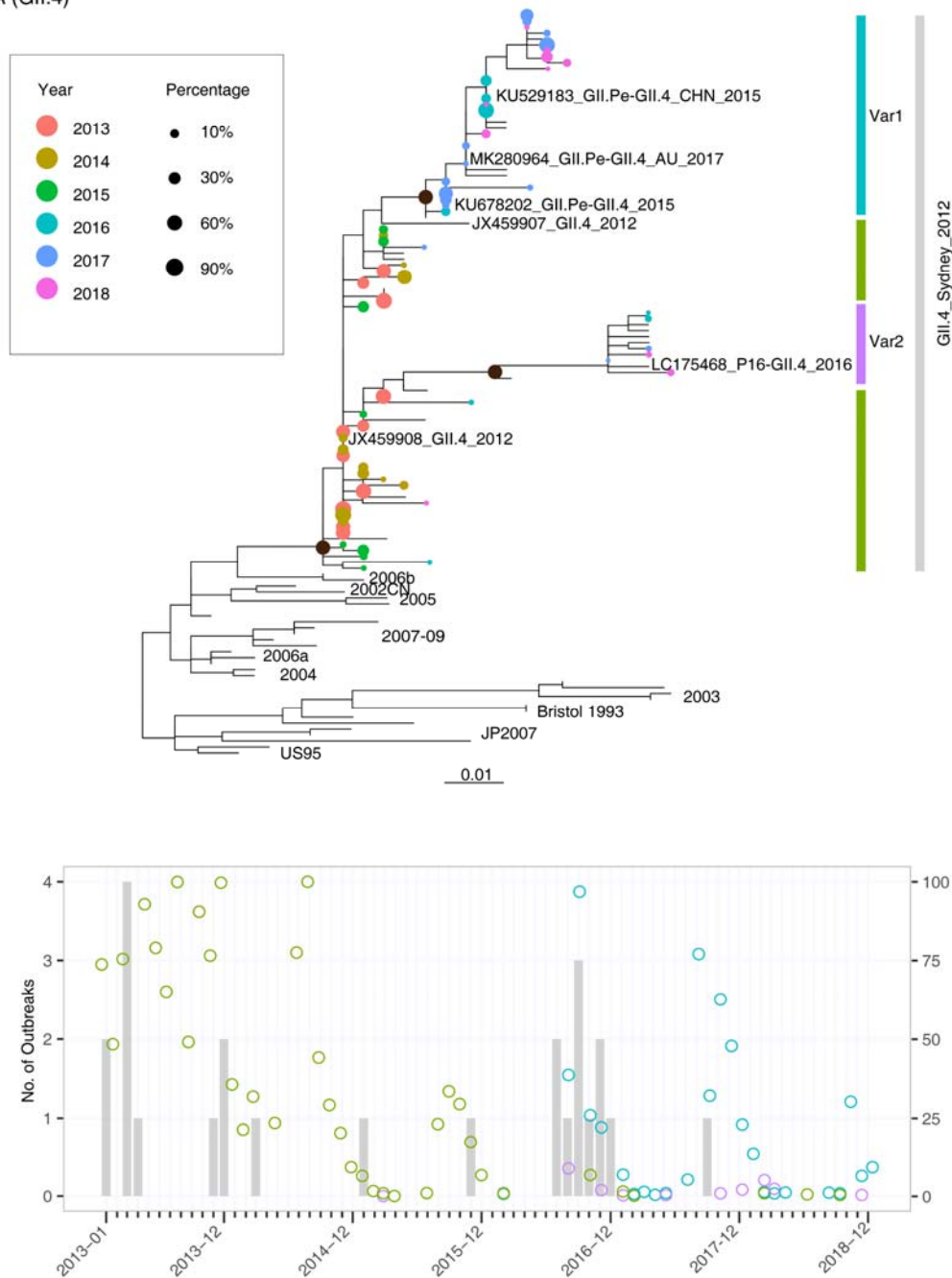
C



526

527 **Fig. 3. Distributions of norovirus genotypes in sewage samples.** Annual distribution (A) and  
 528 monthly distribution (B) of different GI genotypes in sewage samples, January 2013–December 2018.  
 529 Annual distribution (C) and monthly distribution (D) of different GII genotypes, January  
 530 2013–December 2018.

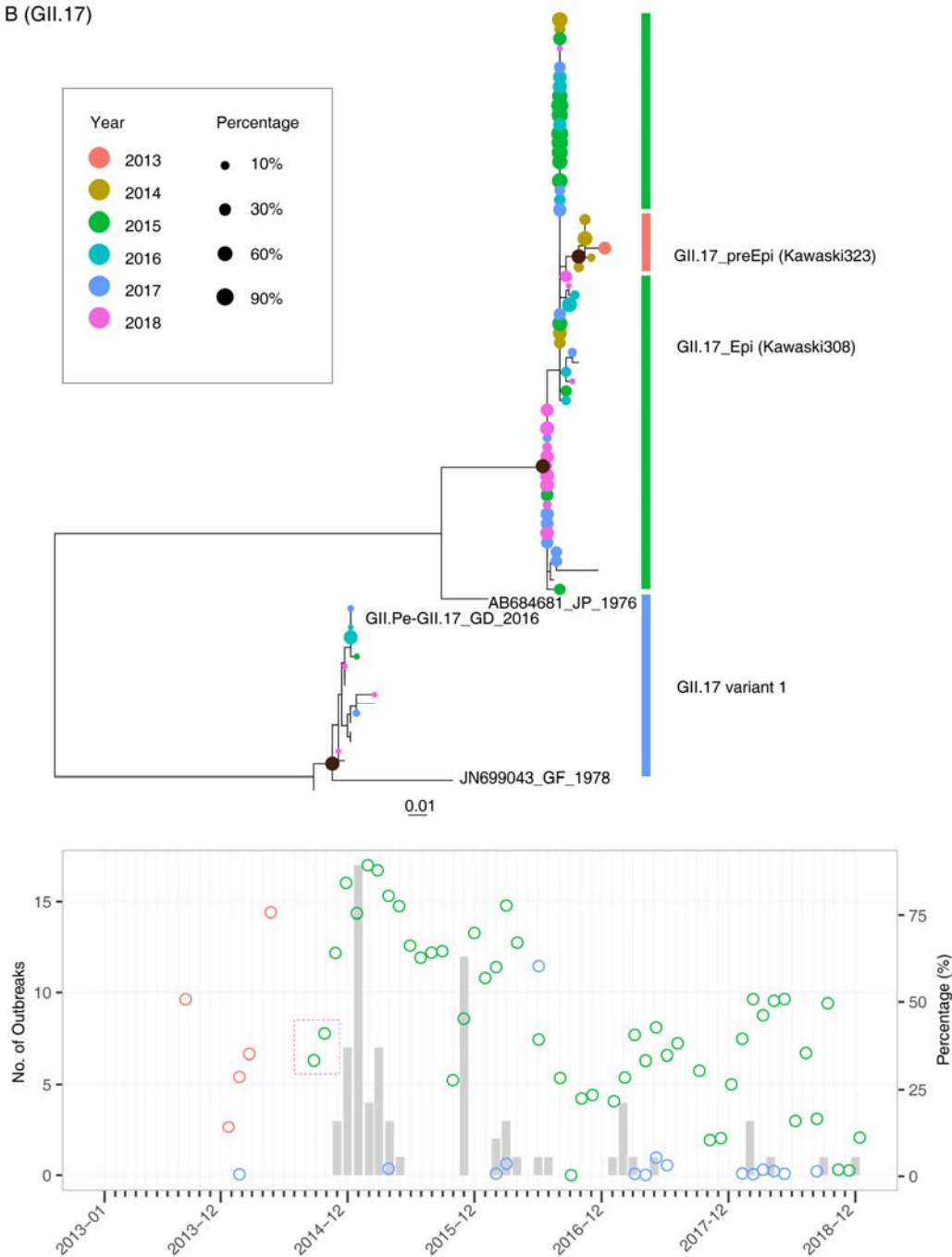
A (GII.4)



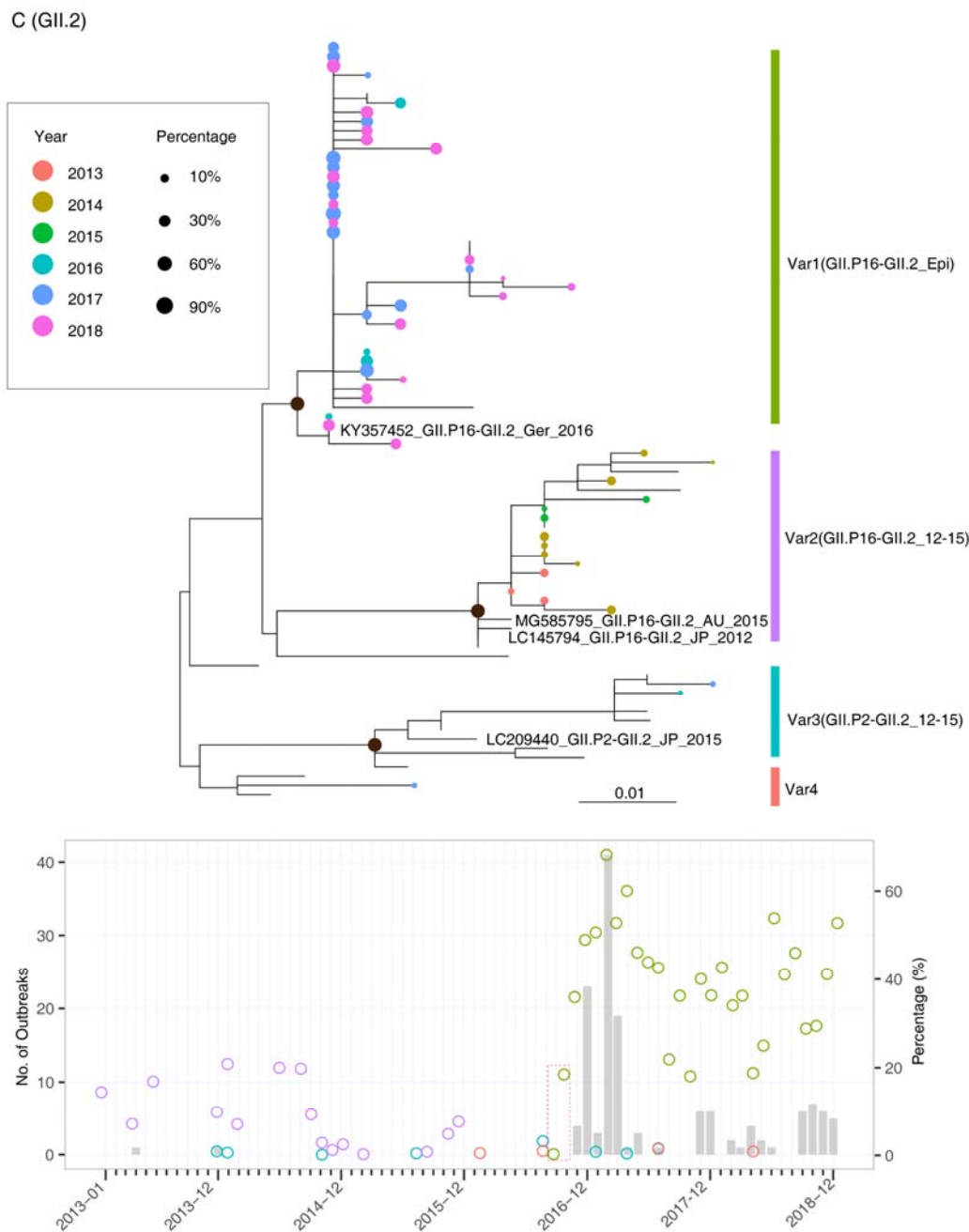
531

532

B (GII.17)



533



534

535 **Fig. 4. Phylogenetic analysis of different genetic variants and their dynamic changes in sewage**

536 **from January 2013 to December 2018.** Upper panel: maximum-likelihood trees were constructed by

537 using the consensus sequences generated from OTU clusters of GII.4 (A), GII.17 (B), and GII.2 (C).

538 The tip points are colored according to the year in which the samples were collected, and the size of the

539 points was adjusted according to their abundances in sewage samples. Lower panel: The percentages of

540 different genetic variants in sewage are plotted with circles, which are colored according to the clusters

541 defined in the phylogenetic trees. The early detection of novel genetic variants in sewage was

542 highlighted with a red box.

543 **Supplementary Materials**

**Table S1 The primer set used in the PCR amplification**

	Primer*	Seq (5' to 3')	Orientation
	COG1F	CGYTGGATGCGNTTYCATGA	Forward
GI	G1SKF	CTGCCCGAATTYGTAATGA	Forward
	G1SKR	CCAACCCARCCATTRTACA	Reverse
	COG2F	CARGARBCNATGTTYAGRTGGATGAG	Forward
GII	G2-SKF	TGGGAGGGCGATCGCAA	Forward
	G2SKR	CCWCCNGCATRHCCRTRTACAT	Reverse

544 \*Primers are set according to the previous publication with a few modifications (46).

545

546 **Table S2 Reads numbers of NoV collected from sewage sample in 2013-2018**

547

548 **Fig. S1. Maximum Likelihood tree of GII.4.** The accession numbers of reference sequences and the  
549 name of sequences recovered from different sewage samples have been noted. The tree was annotated  
550 with the same scheme in Fig. 4A.

551

552 **Fig. S2. Maximum Likelihood tree of GII.17.** The accession numbers of reference sequences and  
553 the name of sequences recovered from different sewage samples have been noted. The tree was  
554 annotated with the same scheme in Fig. 4B.

555

556 **Fig. S3. Maximum Likelihood tree of GII.2.** The accession numbers of reference sequences and the  
557 name of sequences recovered from different sewage samples have been noted. The tree was annotated  
558 with the same scheme in Fig. 4C.

559